Translation-Invariant Multiwavelets for Image De-noising

TIEN DAI BUI, CHEN GUANYI, YVES ROY
Department of Computer Science
Concordia University
1455 De Maisonneuve West, Montreal, Quebec, H3G 1M8
CANADA
bui@cs.concordia.ca, guang_c@cs.concordia.ca, roy@cs.concordia.ca

Abstract: - Over the past decade wavelet transforms have received a lot of attention from researchers in many different areas. Both discrete and continuous wavelet transforms have shown great promises in such diverse fields as image compression, image de-noising, signal processing, computer graphics, and pattern recognition. Most of the work has been done on scalar wavelets. In this paper, we investigate translation-invariant (TI) multiwavelts in image de-noising. The complexity of our TI multiwavelet algorithm is $O((n \log n)^2)$, where the image dimension is $n \times n$. We conduct our experiments by using different threshold values for soft thresholding.

Key-Words: Image de-noising, multiwavelets, translation-invariance, soft thresholding.

1 Introduction

The restoration and enhancement of degraded images are of fundamental importance in image processing applications. Images can be corrupted by various noise processes such as additive Gaussian noise due to a noisy sensor, lossy compression, and transmission over noisy channels.

The non Translation Invariant(TI) image de-noising is realized by decomposing the noisy image into a multiresolution wavelet representation and performing a soft-thresholding to remove the truncation artifacts. The final image is obtained by applying inverse wavelet transform on the threshold wavelet domain image. It should be noted that even though the derivation of wavelet shrinkage method is based on the Gaussian assumption, it can also be applied to non-Gaussian noise except that the threshold value in this case is not asymptotically optimal. This thresholding method has various optimal properties, such as smoothness and adaptation, over a wide range of spaces.

Translation-Invariant(TI) scalar wavelets play an important role in signal and image de-noising([2], [12]). For signals, Coifman and Donoho [2] proposed a TI de-noising scheme to suppress artifacts by averaging over the de-noised signals of all circular shifts. Their experimental results confirmed that scalar TI wavelet de-noising performs better than non-TI scalar wavelet de-noising for 1-D signals. Yu et al [12] extended Coifman and Donoho's approach to 2-D and 3-D TI wavelet de-noising. Also, directional invariant scalar wavelet transform was discussed in [12].

Multiwavelets have recently been developed by using translates and dilates of more than one mother wavelet functions ([8]-[11]). They are known to have several advantages over scalar wavelets such as short support, orthogonality, symmetry, and higher order of vanishing moments. Strela *et al.* [8] claimed that multiwavelet soft thresholding offers better results than the traditional scalar wavelet soft thresholding. Since scalar TI wavelet de-noising also has better performance than the traditional scalar wavelet de-noising, it is natural to attempt TI multiwavelet de-noising and compare the results with scalar TI wavelet

de-noising.

The organisation of this paper is as follows. Section 2 gives a short introduction to multiwavelets. Section 3 explains how TI multiwavelet de-noising works. And finally section 4 shows some experimental results.

2 Discrete Multiwavelet Transform

Multiwavelet basis uses translations and dilations of $L \geq 2$ scaling functions $\{\varphi_k(x)\}_{1\leq k\leq L}$ and L mother wavelet functions $\{\psi_k(x)\}_{1\leq k\leq L}$. If we write $\Phi(x) = (\varphi_1(x),\ \varphi_2(x),\ \ldots,\ \varphi_L(x))^T$ and $\Psi(x) = (\psi_1(x),\ \psi_2(x),\ \ldots,\ \psi_L(x))^T$, then we have

$$\Phi(x) = 2\sum_{k=0}^{2N-1} H_k\,\Phi(2x-k), \tag{1}$$

and

$$\Psi(x) = 2\sum_{k=0}^{2N-1} G_k\,\Phi(2x-k). \tag{2}$$

where $\{H_k\}_{0\leq k\leq 2N-1}$ and $\{G_k\}_{0\leq k\leq 2N-1}$ are $L\times L$ filter matrices.

As an example, we give the most commonly used multiwavelets developed by Geronimo, Hardin and Massopust [7]. Let

$$H_0 = \begin{pmatrix} 3/10 & 2\sqrt{2}/5 \\ -\sqrt{2}/40 & -3/20 \end{pmatrix}, H_1 = \begin{pmatrix} 3/10 & 0 \\ 9\sqrt{2}/40 & 1/2 \end{pmatrix},$$
$$H_2 = \begin{pmatrix} 0 & 0 \\ 9\sqrt{2}/40 & -3/20 \end{pmatrix},\ H_3 = \begin{pmatrix} 0 & 0 \\ -\sqrt{2}/40 & 0 \end{pmatrix},$$

and

$$G_0 = \begin{pmatrix} -\sqrt{2}/40 & -3/20 \\ -1/20 & -3\sqrt{2}/20 \end{pmatrix}, G_1 = \begin{pmatrix} 9\sqrt{2}/40 & -1/2 \\ 9/20 & 0 \end{pmatrix},$$
$$G_2 = \begin{pmatrix} 9\sqrt{2}/40 & -3/20 \\ -9/20 & 3\sqrt{2}/20 \end{pmatrix}, \quad G_3 = \begin{pmatrix} -\sqrt{2}/40 & 0 \\ 1/20 & 0 \end{pmatrix}.$$

then the two functions $\varphi_1(x)$ and $\varphi_2(x)$ can be generated via (1). Similarly, the two mother wavelet functions $\psi_1(x)$ and $\psi_2(x)$ can be constructed by (2).

Let V_J be the closure of the linear span of $2^{J/2}\phi_l(2^Jt-k), l = 1,2; k \in Z$. With the above constructions, it has been proved that $\phi_l(t-k), l = 1,2; k \in Z$ form an orthonormal basis for V_0, and moreover the dilations and translations $2^{j/2}\psi_l(2^j - k), l = 1,2; j,k \in Z$ form an orthonormal basis for $L^2(R)$. In other words, the spaces $V_j, j \in Z$, form an orthogonal multiresolution analysis of $L^2(R)$. Let

$$H(w) = \sum_{k=0}^{3} H_k e^{iwk}, \tag{3}$$

$$G(w) = \sum_{k=0}^{3} G_k e^{iwk}. \tag{4}$$

From the orthogonality, we have

$$H(w)H^T(w) + H(w+\pi)H^T(w+\pi) = I_2 \tag{5}$$
$$G(w)G^T(w) + G(w+\pi)G^T(w+\pi) = I_2 \tag{6}$$
$$H(w)G^T(w) + H(w+\pi)G^T(w+\pi) = 0_2 \tag{7}$$

where ^{T} means the complex conjugate transpose, I_2 and 0_2 denote the 2×2 identity and all zero matrix, respectively. Let $f \in V_0$, then

$$\begin{aligned} f(t) &= \sum_{k\in Z}(c_{1,0,k}\phi_1(t-k) + c_{2,0,k}\phi_2(t-k)) \\ &= \sum_{k\in Z}(c_{1,J_0,k}2^{J_0/2}\phi_1(2^{J_0}t-k) \\ &\quad + c_{2,J_0,k}2^{J_0/2}\phi_2(2^{J_0}t-k)) \\ &\quad + \sum_{J_0\leq j<0}\sum_{k\in Z}(d_{1,j,k}2^{j/2}\psi_1(2^jt-k) \\ &\quad + d_{2,j,k}2^{j/2}\psi_2(2^jt-k)) \end{aligned} \tag{8}$$

where

$$c_{i,j,k} = \int f(t)2^{j/2}\phi_i(2^jt-k)dt \tag{9}$$

$$d_{i,j,k} = \int f(t)2^{j/2}\psi_i(2^jt-k)dt \tag{10}$$

for $i = 1,2; j,k \in Z$ and $J_0 < 0$. By the dilation equations, we have the following recursive relationship between the coefficients $(c_{1,j,k}, c_{2,j,k})^T$ and $(d_{1,j,k}, d_{2,j,k})^T$:

$$\begin{pmatrix} c_{1,j-1,k} \\ c_{2,j-1,k} \end{pmatrix} = \sqrt{2}\sum_{l=0}^{3} H_l \begin{pmatrix} c_{1,j,2k+l} \\ c_{2,j,2k+l} \end{pmatrix}, \quad j,k \in Z \tag{11}$$

and

$$\begin{pmatrix} d_{1,j-1,k} \\ d_{2,j-1,k} \end{pmatrix} = \sqrt{2}\sum_{l=0}^{3} G_l \begin{pmatrix} d_{1,j,2k+l} \\ d_{2,j,2k+l} \end{pmatrix}, \quad j,k \in Z \tag{12}$$

Moreover,

$$\begin{aligned} \begin{pmatrix} c_{1,j,l} \\ c_{2,j,l} \end{pmatrix} = \sqrt{2}\sum_{k=0}^{3}\Bigg(H_k^T \begin{pmatrix} c_{1,j-1,2k+l} \\ c_{2,j-1,2k+l} \end{pmatrix} \\ + G_k^T \begin{pmatrix} d_{1,j-1,2k+l} \\ d_{2,j-1,2k+l} \end{pmatrix}\Bigg). \end{aligned} \tag{13}$$

Multiwavelets have some advantages in comparison to scalar ones. For example, such features as short support, orthogonality, symmetry, and higher order of vanishing moments, are known to be important in signal processing. A scalar wavelet cannot possess all these properties at the same time. Therefore, multiwavelets can give better results than the scalar wavelets in image compression and de-noising [8].

3 TI Multiwavelet De-noising

The algorithm for TI multiwavelet de-noising is quite similar to the case for TI scalar wavelet de-noising. The noisy image is transformed into multiwavelet domain by applying TI GHM multiwavelets along the rows and columns, respectively. Because the GHM multiwavelet transform needs two rows for the input, we group two adjacent rows when we do the transform along row and two adjacent columns when transforming along columns. A soft or hard thresholding is applied to the resulting multiwavelet coefficients. In order to get the de-noised image, we perform inverse multiwavelet transform along the columns and rows, respectively.

At the first glance, this proposal seems to be impractical because a naive implementation of the method increases the complexity of wavelet shrinkage algorithm from $O(n^2)$ to $O(n^4)$ for $n \times n$ images. Fortunately, the $O(n \log n)$ fast algorithm in 1-D can easily be generalised to 2-D case so that the algorithm can be implemented with $O((n \log n)^2)$ complexity.

Both the soft (shrink or kill) and the hard (keep and kill) thresholding methods compare the input to a given threshold and set it to zero if its magnitude is less than the threshold. The idea is that coefficients insignificant relative to the threshold are likely due to noise, whereas significant coefficients are important signal structures. Thresholding essentially creates a region around zero where the coefficients are considered negligible. Outside this region, the threshold are kept to full precision.

The choice of the threshold is critical in wavelet shrinkage. If it is too small or too big then the wavelet shrinkage estimator will tend to overfit or underfit the data. Donoho and Johnstone(1994) proposed the universal threshold $\sigma\sqrt{2 \log n}$ where n is the number of points in the signal. Despite the simplicity of such a threshold, they showed that the resulting nonlinear wavelet estimator is spatially adaptive and is asymptotically near-minimax within the whole range of Besov spaces. In the case of image de-noising the threshold can be adjusted to be $\sigma\sqrt{2 \log n^2} = 2\sigma\sqrt{\log n}$. However, as we shall see in the next section, this threshold is far too big for image de-noising.

4 Experimental Results

We explore the applications of the TI multiwavelet transform in image de-noising. In order to compare the results with other papers, we use the famous image, Lenna, in our experiments. The dimension of the image is 256×256 pixels with each pixel having a gray level ranging from 0 to 255. The multiple wavelets used in our experiments is the GHM multiwavelets. Even though hard thresholding can be used in the thresholding process, we only use soft thresholding. The reason for this is that hard thresholding does not perform as well as soft thresholding in our previous experiments for signal de-noising [1].

Figure 1 shows some images obtained by using our proposed algorithms. There are three rows in Figure 1. The first row has a SNR= $2dB$, the second row has a SNR= $5dB$, while the third row has a SNR= $10dB$. For each row we have four images numbered (a) to (d). Image (a) is the noisy image produced by adding white noises onto the original clean image. Images (b) to (d) are the images restored by using our algorithm with threshold equal to 1.5, 2.5, and 5, respectively. It is clear that the theoretical threshold $2\sigma\sqrt{\log n}$ is too big for this kind of application. We find that a threshold of 1.5 gives nearly minimal mean square error(MSE) in Table 1.

5 Conclusion

In this paper we discuss and implement an algorithm for image de-noising using TI multiwavelets. Experimental results show that the TI multiwavelet de-noising gives better results than the conventional TI scalar wavelet de-noising. Also, the TI

SNR	*Soft Thresholds*					
	1.5	*2.0*	*2.5*	*3.0*	*4.0*	*5.0*
2	17.5	19.9	22.6	25.2	29.7	33.5
3	13.8	15.9	18.3	20.5	23.9	27.0
4	11.7	13.6	10.3	17.7	20.9	23.4
5	10.6	12.2	13.9	15.7	18.8	21.1
10	10.9	11.7	12.2	12.9	14.3	15.9
20	9.7	10.6	11.1	11.2	11.6	12.1

Table 1: MSE for TI de-noising for different thresholds and Signal-to-Noise Ratio(SNR)

SNR	Soft Thresholds					
	1.5	*2.0*	*2.5*	*3.0*	*4.0*	*5.0*
2	21.8	23.8	25.9	27.7	31.0	33.6
3	16.8	19.3	21.4	23.4	26.2	28.5
4	13.6	15.8	17.9	19.9	23.2	25.4
5	11.9	13.7	15.6	17.4	20.5	23.1
10	10.4	10.6	11.1	12.0	14.1	15.9
20	10.3	10.9	10.9	10.9	11.4	12.0

Table 2: MSE for Non-TI de-noising for different thresholds and Signal-to-Noise Ratio (SNR)

multiwavelets perform better than the non-TI multiwavelets in our experiments for image de-noising. Furthermore, er also found that the theoretical threshold in [4] is too big for this kind of applications.

Acknowledgements

This work was supported by research grants from the Natural Sciences and Engineering Research Council of Canada and by the Fonds pour la Formation de Chercheurs et l'Aide à la Recherche of Quebec.

References:

[1] T. D. Bui and C. Guangyi, "Translation invariant de-noising using multiwavelets" In *IEEE Trans. on Signal. Processing*, Vol.46, No.12, 1998, pp. 3414-3420.

[2] R. R. Coifman and D. L. Donoho, "Translation invariant denoising," In *Wavelets and Statistics, Springer Lecture Notes in Statistics 103*, pp. 125-150, New York:Springer-Verlag.

[3] D. L. Donoho, "De-noising by soft-thresholding," *IEEE Trans. Inf. Theory*, Vol.41, 1995, pp. 613-627.

[4] D. L. Donoho and I. M. Johnstone, "Ideal spatial adaptation via wavelet shrinkage" *Biometrika*, Vol.81, 1994, pp. 425-455.

[5] D. L. Donoho, I. M. Johnstone, G. Kerkyacharian, and D. Picard, "Wavelet shrinkage: Asymptopia?" *Journal of the Royal Statistics Society, Series B*, Vol.57, 1995, pp. 301-369.

[6] T. R. Downie and B. W. Silverman, "The discrete multiple wavelet transform and thresholding methods," Technical Report, Department of Mathematics, University of Bristol, University Walk, Bristol, BS8 1TW, U.K., 1996.

[7] J. S. Geronimo, D. P. Hardin, and P. R. Massopust, "Fractal functions and wavelet expansions based on several scaling functions," *Journal of Approximation Theory*, Vol.78, 1994, pp. 373-401.

[8] V. Strela, P. N. Heller, G. Strang, P. Topiwala, and C. Heil, "The application of multiwavelet filter banks to image processing," Technical report, MIT, USA, 1995.

[9] G. Strang and V. Strela, "Orthogonal multiwavelets with vanishing moments," *Optical Engineering*, Vol.33, 1994, pp. 2104-2107.

[10] G. Strang and V. Strela, "Short wavelets and matrix dilation equations," *IEEE Trans. on Signal Processing*, Vol.43, 1995, pp. 108-115.

[11] X. G. Xia, J. Geronimo, D. Hardin, and B. Suter, "Design of prefilters for discrete multiwavelet transforms," *IEEE Trans. on Signal Processing*, Vol.44, 1996, pp. 25-35.

[12] Thomas P. Y. Yu, Arne Stoschek, and David L. Donoho, "Translation- and direction-invariant de-noising of 2-D and 3-D images: experience and algorithms," in *Wavelet Applications in Signal and Image Processing IV, Proceedings SPIE'96*.

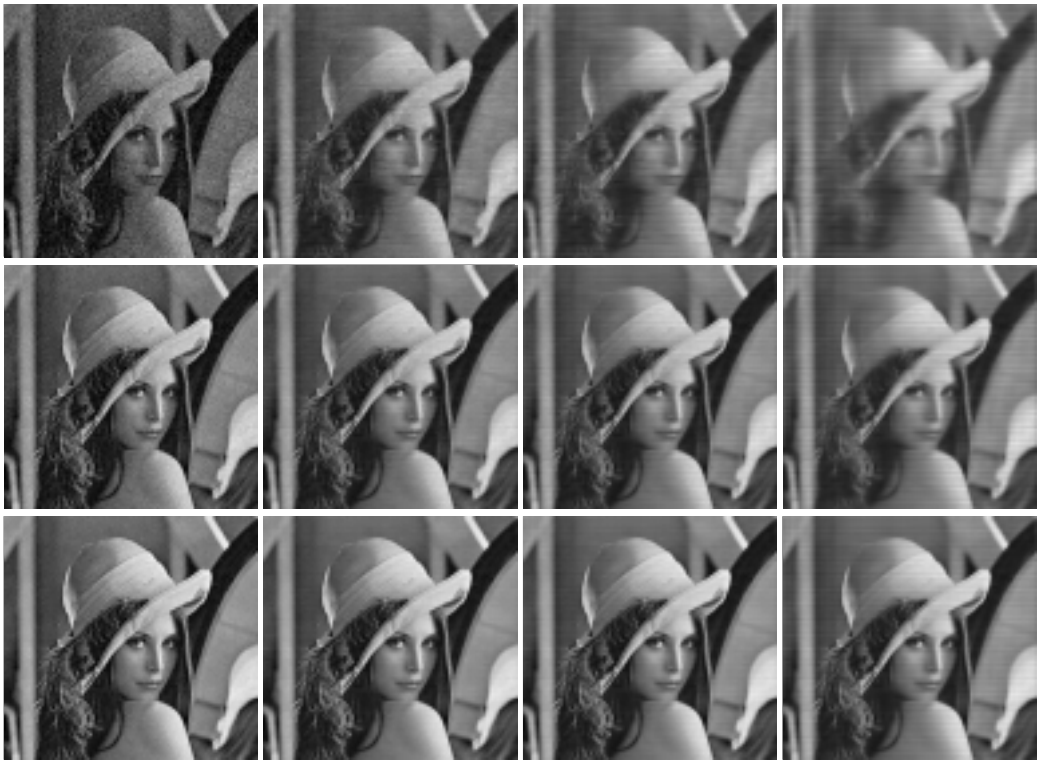

(a) Noisy Image | (b) THR = 1.5 | (c) THR = 2.5 | (d) THR = 5.0

Figure 1: Experimental results for different SNR's and thresholds with TI de-noising. The SNR's for row 1, 2 and 3 are $2dB$, $5dB$ and $10dB$, respectively. (a) Noisy image with Gaussian noise added (b) De-noised image with soft threshold 1.5 (c) De-noised image with soft threshold 2.5 (d) De-noised image with soft threshold 5.0